Supplemental material

Table S1: Minimal inhibitory concentrations against different strains.

Strains	Nisin	Subtilin	Nisin$_{1-17}$-Subtilin$_{18-32}$
Kocuria rhizophila (ATCC 9341)	~3-6 nM	~3-6 nM	~6-12 nM
L. lactis MG1614	~75 nM	~38 nM	Not determined.
B. subtilis 168	~150 nM	~300 - 600 nM	~310 - 620 nM

*MIC values are provided in nM concentrations

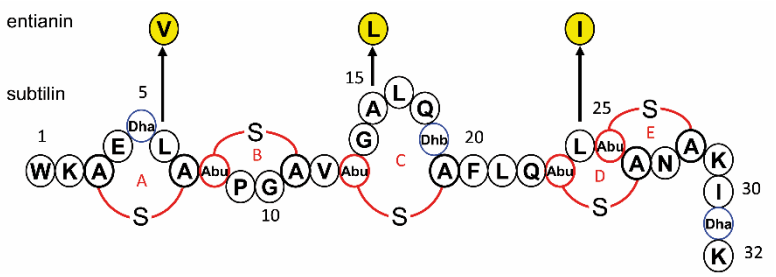

FIG S1: Structures and amino acid sequences of subtilin-like lantibiotics. Differences between subtilin and entianin are highlighted in yellow. A-S-A, meso-lanthionine; Abu-S-A, 3-methyl-lanthionine; Abu, α-aminobutyric acid; Dha, 2,3-didehydroalanine; Dhb, 2,3-didehydrobutyrine.

Sequence-alignment of lipoproteins SpaI and NisI

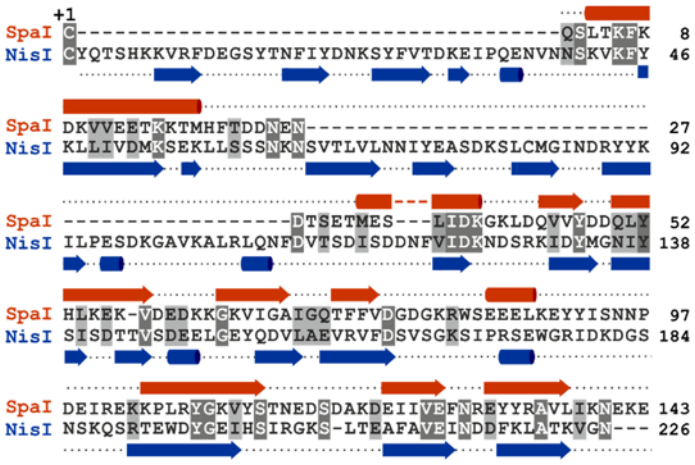

FIG S2: Sequence-alignment of SpaI and NisI with secondary structure elements. Residue numbers are indicated on the right; arrows: β-sheets; cylinder: α-helices; different shades of grey indicate degree of similarities.

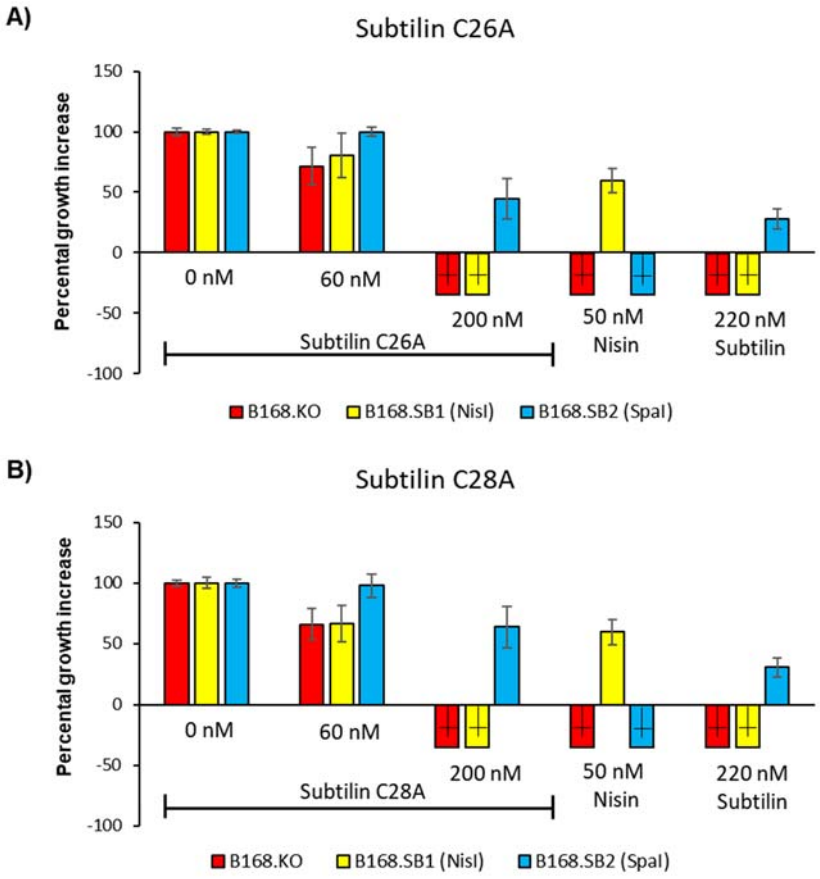

FIG S3: NisI and SpaI mediated immunity against subtilin ring disruption mutants C26A and C28A. Percental growth increase after 0.5 h incubation with subtilin C26A (A) and C28A (B) normalized to a control without lantibiotic (red: Control strain B168.KO without immunity, yellow: NisI expression strain B168.SB1 and blue: SpaI expression strain B168.SB2). The hatched bars indicate a decrease in optical density presumable due to cell lysis.

Immunity mediation of SpaFEG and SpaIFEG after nisin addition

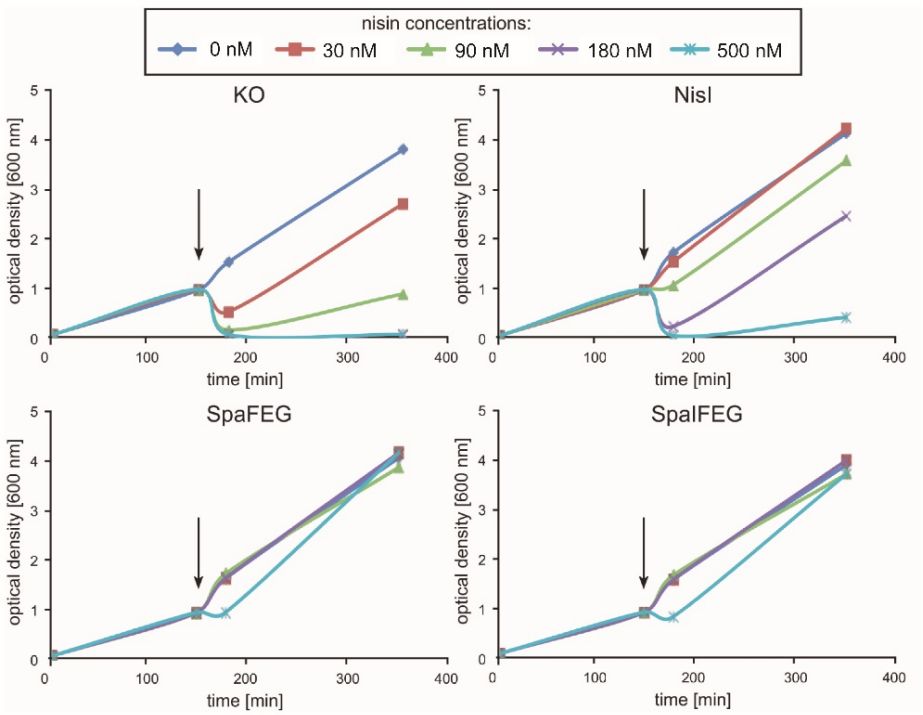

FIG. S4: Immunity mediated by NisI, SpaFEG and SpaIFEG. Growth curves of strains B168.KO (KO – w/o immunity proteins), B168.SB1 (NisI), B2470.TM1 (SpaFEG) and B2470.TM2 (SpaIFEG) after addition of different nisin concentrations. Arrows indicate the time point of nisin addition.

The comparison of the growth behavior of the control strain (B168.KO) without immunity and the NisI expressing strain (B168.SB1) after nisin addition bears significant differences. While the control strain already showed growth deficits at nisin concentrations of 30 nM, similar effects on the NisI expression strain only became apparent at 90 nM thus verifying the protective effect of NisI against nisin. Interestingly, the SpaFEG (B2470.TM1) as well as the SpaIFEG expressing strain (B2470.TM2) showed a significantly increased tolerance to nisin, whereas the single expression of the SpaI protein had no increasing effect on the immunity at all. The *B. subtilis* ABC-transporter SpaFEG mediated an even higher immunity level compared to NisI. While the latter one only tolerated nisin concentrations of 90 nM SpaFEG is able to tolerate concentrations up to 500 nM. Since it was assumed that the immunity mechanisms of

the lantibiotics are highly specific for the own synthesized peptide, this result becomes even more interesting.

LILBID measurement of SpaI$_{18-143}$ with nisin Z

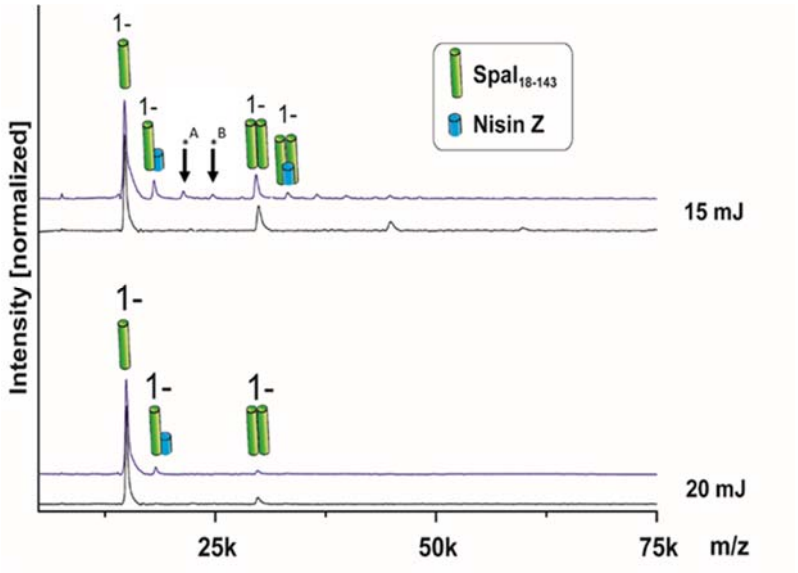

FIG S5: LILBID analysis of the interaction between the truncated immunity protein SpaI$_{18-143}$ and class I lantibiotic nisin Z. Compendium of the measurements of SpaI$_{18-143}$ (black) and SpaI$_{18-143}$ + nisin Z (blue). Shown spectra were recorded at low (15 mJ) and high (20 mJ) laser intensities. Instrumental settings as well as protein concentrations were identical for all measurements. Nisin Z was applied in 3-fold excess (48 µM) over SpaI (16 µM). Spectra are averaged out of 1,000 single measurements. Arrows mark signals/masses that could be assigned to the monomer of SpaI with two ($*^{A}$) or even three nisin molecules ($*^{B}$).